Cal Poly State University
San Luis Obispo

A Senior Project

---

# The Double Pendulum:
## Construction and Exploration

---

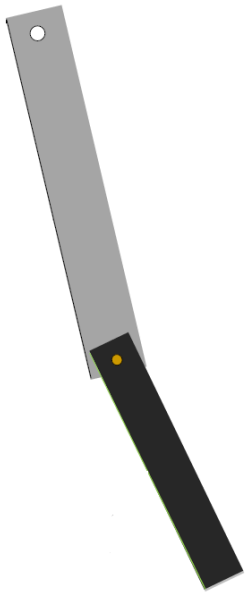

Benjamin J Knudson

July 4, 2012

Approval Page

Title: The Double Pendulum: Construction and Exploration
Author: Benjamin J Knudson
Date Submitted: July 4, 2012

Senior Project Advisor: Dr. Matthew J Moelter

_____
Signature

_____
Date

# Contents

# List of Figures

# List of Tables

# Chapter 1

# Introduction

## 1.1 About This Document

As the author, I forsee you, the reader, having one of three interests in this project write-up. The first and most likely interest is academic; you wish to assign a letter grade to my efforts on this project and "grading" this report is the most formal way to do so. You must read every word, and for that you earn kudos! Optimistically, the second interest is that you have a practical interest in the Double Pendulum, the apparatus whose design, construction, use, and characterization are outlined below. You may feel free to hop directly to the section of interest, if you haven't already. Lastly, I realize that some of my friends and family may want to see what I've been doing in my lab for some time now. This group may prefer a little flowery language and then just look at the pretty pictures. This last group may benefit from the following description:

> What is a Double Pendulum? It's a pendulum on a pendulum. Imagine the pendulum of a grandfather clock with a lovely swinging bob that Edgar Allen Poe would love to write about. Now put another pendulum on that pendulum. This takes the zombie-like theme of slow inevitable death and adds a wild twist.

> Poe might be shaken since the rhythmic and repetitive motion of his pendulum is replaced by a strikingly chaotic and scary motion. Why scary? Because it's unpredictable; it doesn't (or doesn't appear to) follow any set patterns. A victim in Poe's updated poem of death due to a double pendulum razor would find it surprising when and how the razor finally meets its mark.

With the romanticism overwith, the remainder of this paper is academic and includes an introduction into nonlinear dynamics and chaos (1.2), a detailed analytical attempt at solving the double pendulum (2.2) with accurate characterization (2.3), discussion of the design and construction of the double pendulum (3), and details for successful operation of the double pendulum apparatus using Vernier LabPro and LoggerPro (4.2).

## 1.2 Linear vs Nonlinear Dymanics

The world of dynamical systems can be divided into two categories: systems that can be solved analytically and systems that cannot. The latter group is much larger than the former. These systems are selfreferential and in math speak that means they are differential equations. In general, linear differential systems, systems in the form of equation 1.1 or 1.2 where the functions $f()$ and $g()$ are linear polynomials, are solvable. For example, a mass-spring system described by $\ddot{x} = -\frac{k}{m}x$ is solvable and yields the position equation $x(t) = Ae^{i\sqrt{\frac{k}{m}}t}$, the real part of which describes the physical osillations of the mass on the spring, $x(t) = A\cos(\sqrt{\frac{k}{m}}t + \delta)$, where $\delta$ and $A$ are constants determined by the initial conditions.

$$\dot{\vec{x}}(t) = f(\vec{x}(t), \dot{\vec{x}}(t), t) \quad \text{first order} \tag{1.1}$$

$$\ddot{\vec{x}}(t) = g(\vec{x}(t), \dot{\vec{x}}(t), t) \quad \text{second order} \tag{1.2}$$

The mass-spring system is solvable because of the convenience of $\frac{d}{dt}e^x = \frac{dx}{dt}e^x$. But what about nonlinear systems? A simple pendlum with the equation of motion

$$\ddot{\theta} = -\frac{g}{l}\sin\theta, \tag{1.3}$$

however, is unsolvable because the second derivative of sin() is not itself but $-\sin()$. (But wait, we used an imaginary number to change the sign of the function in the mass-spring system, does that work here? No, the imaginary number $\sin(i\sqrt{\frac{g}{l}}t)$ might solve the simple pendulum system, but the solution is entirely imaginary.) The punchline of this example is that nonlinear systems are not analytically solvable like linear systems.

## 1.3 "Solving" Nonlinear Systems

The simple pendulum is not analyitically solvable because the equation of motion is not linear like the mass-spring system, but that does not mean we are out of luck. One strategy is to approximate nonlinear systems as linear systems. This linearization is often accurate within certain boundaries. If we restrict the simple pendulum to small angles ($\theta \approx$ small), then we can approximate $\ddot{\theta}$ using the approximation $\sin\theta \approx \theta$. This makes Equation 1.3 become $\ddot{\theta} = -\frac{g}{l}\theta$, which has solutions similar to the mass-spring system. The only way to avoid approximations such as this one, is by employing the use of a computer to solve these equations of motion numerically. This method is not outlined here, but the characteristics in Table 2.1 would aid someone who wished to explore this option.

## 1.4 Chaos

Chaos, as Strogatz [1] suggests, is sensitive dependence on initial conditions. A system that is deterministic, that is to say, if given the same initial conditions and the same time span

will yield the same trajectory, exhibits chaos if the system is sufficiently sensitive to initial conditions that the same trajectory is not reproducible. Seemingly similar conditions yield a different trajectory and often a different end state (if the system has more than one fixed point). In all practical cases of chaos, a physical or computational chaotic system will not have enough accuracy to produce two of the same (or similar) trajectories consistently due to variations in the system and rounding errors. Some examples of chaos are included in Appendix B.

Chaos should not be confused with randomness. The difference is simple: A random system should *not* yield similar trajectories but *might*, and a chaotic system *should* yield the same trajectory but *doesn't*. Chaos and randomness sometimes go hand-in-hand. The state of a chaotic system at a certain time might be random. The details of the system will determine how random and what type of randomness is expected, for example a system that is similar to a random walk might exhibit a gaussian distribution and a system like a magnetic moment free to move and free of outside fields might produce a uniform probability distribution over its available angular region.

## 1.5 Why a Double Pendulum?

This introduction outlines the best answer to the question, "Why a double pendulum?" A double pendulum exhibits chaos, but is simple enough to approximate and analyze. It is a nonlinear coupled oscillator with complicated motion, but it is relatively simple to interface with a computer. Double pendulums are common in nonlinear investigations and are also studied in classical mechanics classes, therefore, the construction of a reliable and usable apparatus is a benefit to the physics department at Cal Poly as a whole.

# Chapter 2

# Solving the Double Pendulum

## 2.1 The Simple Double Pendulum

Let's first explore the Double Pendulum using a simplified model. Figure 2.1 shows the general and simplified versions of the model. Taylor [2] has a nice treatment of the simple double pendulum shown in Figure 2.1b. Taylor uses the Lagrangian (Equation 2.1) to determine a system of differential equations of the form given in Equation 2.2

$$L = \frac{1}{2}ml^2\left[2\dot{\phi_1}^2 + 2\dot{\phi_1}\dot{\phi_2}\cos(\phi_1 - \phi_2) + \dot{\phi_2}^2\right] - 2mgl(1-\cos\phi_1) - mgl(1-\cos\phi_2) \quad (2.1)$$

$$\mathbf{M}\ddot{\vec{\phi}} = -\mathbf{K}\vec{\phi}, \quad (2.2)$$

where $\mathbf{M}$ is a matrix of numbers/parameters that correspond to inertia and $\mathbf{K}$ is a matrix of numbers/parameters that correspond to energy storage (much like the $m$ and $k$ of a mass on a spring system). In order to solve this system analyitically, the small angle approximation must be used. We assume $\phi_1$, $\phi_2$, $\dot{\phi_1}$, and $\dot{\phi_1}$ are all small. In the Lagrangian in Equation 2.1, we approximate the term $\cos(\phi_1 - \phi_2) \approx 1$ since it is multiplied by the double small quantity $\dot{\phi_1}\dot{\phi_2}$. The cosines in the potential energy terms are then expanded and the first

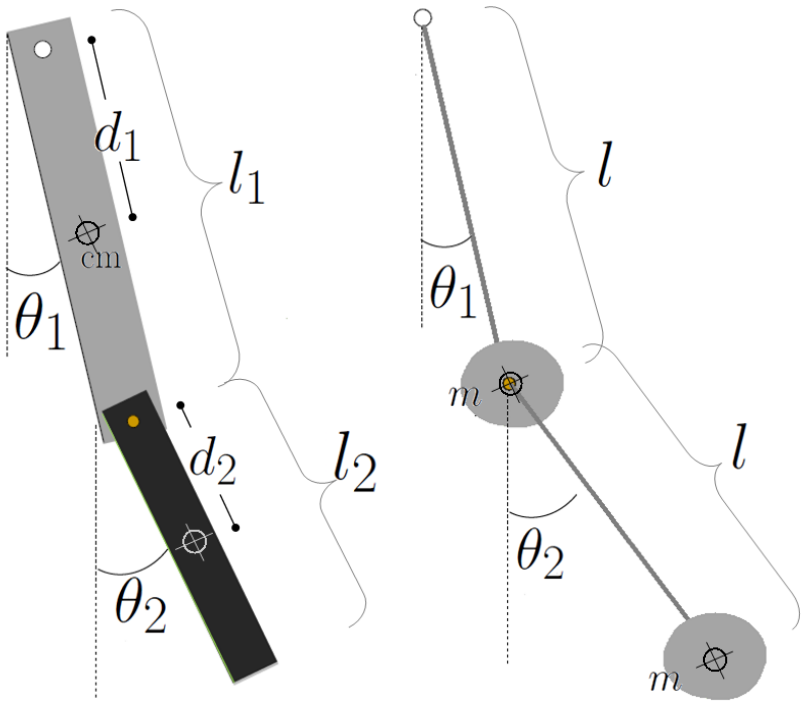


(a) General (b) Simple

Figure 2.1: (a) The general schematic of the Double Pendulum. To fully describe the pendulum, we need to include the masses, $m_1$ and $m_2$, and the moments of inertia, $I_1$ and $I_2$, of the two arms which may be different. (b) The simple double pendulum schematic assumes all the mass to be located at the bobs and the connecting rigid rods are massless.

two terms are used ($\cos\phi \approx 1 - \frac{\phi^2}{2}$) to get Equation 2.3. This yields the system of equations corresponding to Equation 2.2 that can be solved analytically.

$$L = \frac{1}{2}ml^2\left[2\dot{\phi_1}^2 + 2\dot{\phi_1}\dot{\phi_2} + \dot{\phi_2}^2\right] - mgl\phi_1^2 - \frac{1}{2}mgl\phi_2^2. \tag{2.3}$$

The Lagrangian yields the system in Equation 2.4,

$$\begin{aligned} 2ml^2\ddot{\phi_1} + ml^2\ddot{\phi_2} &= -mgl\phi_1 \\ ml^2\ddot{\phi_1} + ml^2\ddot{\phi_2} &= -mgl\phi_2 \end{aligned} \tag{2.4}$$

which has the form of Equation 2.2.

### 2.1.1 Normal Modes

Now that we have the system, we can proceed to find the normal modes. These modes, then, can be combined to form any motion of the pendulum assuming our approximations still hold. The normal mode frequencies, the eigenvalues ($\omega^2$), are determined by solving $\det(\mathbf{K} - \omega^2\mathbf{M}) = 0$ and are given by the solutions of a quadratic which yields

$$\omega^2 = (2 \pm \sqrt{2})\frac{g}{l}. \tag{2.5}$$

Our simplification in Figure 2.1b has one last benefit: we see that the quantity $\frac{g}{l}$ is related to the natural frequency of a simple pendulum ($\omega_0^2$) and therefore Equation 2.5 can be written

$$\begin{aligned} \omega^2 &= (2 \pm \sqrt{2})\omega_0^2 \\ \omega_+ &= \sqrt{2+\sqrt{2}}\ \omega_0 = 1.848\omega_0 \\ \omega_- &= \sqrt{2-\sqrt{2}}\ \omega_0 = 0.765\omega_0. \end{aligned} \tag{2.6}$$

Equation 2.7 is a clean equation for the frequencies of the normal modes of the double pendulum. Trying to suppress our excitement, we solve for the eigenvectors $\vec{a}$ which satisfy $(\mathbf{K} - \omega^2\mathbf{M})\vec{a} = 0$ and represent the magnitudes of the oscillations of each angle ($\phi_1$ and $\phi_2$). For $\omega_+$, we find that $\vec{a}_+ = \begin{pmatrix} 1 \\ -\sqrt{2} \end{pmatrix}$, a mode in which the angles of the bobs are out-of-phase (the amplitude of one is porportional to the negative of the other $A_2 = -\sqrt{2}\ A_1$). And for $\omega_-$, we find that $\vec{b}_- = \begin{pmatrix} 1 \\ \sqrt{2} \end{pmatrix}$, a mode in which the angles of the bobs are in-phase (the amplitude of one is porportional to the other $B_2 = \sqrt{2}\ B_1$). Our general solution for

the motion of the simple double pendulum in Equation 2.7 describes all the motions of the double pendulum within our approximation constraints (small values of $\vec{\phi}$ and $\ddot{\vec{\phi}}$).

$$\vec{\phi} = A \begin{pmatrix} 1 \\ -\sqrt{2} \end{pmatrix} \cos(\omega_+ t) + B \begin{pmatrix} 1 \\ \sqrt{2} \end{pmatrix} \cos(\omega_- t) \tag{2.7}$$

The parameters $A$ and $B$ are unique to the motion and depends on the initial conditions. They tell us its composition, is the motion mostly the $\omega_+$ mode or mostly the $\omega_-$ mode.

## 2.2 The General Case

We can now expand our method to include pendulums with distributed mass such as the pendulum in Figure 2.1a. The Lagrangian changes because the length of the pendulum is no longer the distance to its center of mass ($d \neq l$).

$$\begin{aligned} L = \quad & \tfrac{1}{2} I_1 \dot{\phi}_1^2 + \tfrac{1}{2} m_2 l_1^2 \dot{\phi}_1^2 + \tfrac{1}{2} I_2 \dot{\phi}_2^2 + m_2 d_2 l_1 \dot{\phi}_1 \dot{\phi}_2 \cos(\phi_1 - \phi_2) \\ & -[m_1 g d_1 (1 - \cos\phi_1) + m_2 g l_1 (1 - \cos\phi_1) + m_2 g d_2 (1 - \cos\phi_2)] \end{aligned} \tag{2.8}$$

Then, following the approximations concerning small angles from above, our Lagrangian becomes

$$\begin{aligned} L = \quad & \tfrac{1}{2} I_1 \dot{\phi}_1^2 + \tfrac{1}{2} m_2 l_1^2 \dot{\phi}_1^2 + \tfrac{1}{2} I_2 \dot{\phi}_2^2 + m_2 d_2 l_1 \dot{\phi}_1 \dot{\phi}_2 \\ & -[\tfrac{1}{2} m_1 g d_1 \phi_1^2 + \tfrac{1}{2} m_2 g l_1 \phi_1^2 + \tfrac{1}{2} m_2 g d_2 \phi_2^2]. \end{aligned} \tag{2.9}$$

This general case allows for the pendulums to be quite different. They can have different total masses and lengths as well as mass distributions (therefore different moments of inertia). Following the treatment of the simple case, Equation 2.9 yields a more complicated

system of equations 2.10

$$\begin{aligned}(m_2 l_1^2 + I_1)\ddot{\phi}_1 + m_2 d_2 l_1 \ddot{\phi}_2 &= -(m_1 g d_1 - m_2 g l_1)\phi_1 \\ m_2 d_2 l_1 \ddot{\phi}_1 + I_1 \ddot{\phi}_2 &= -m_2 g d_2 \phi_2 \end{aligned} \tag{2.10}$$

which, when solved using the method in section 2.1.1, yields normal modes like before. These normal mode frequencies are the solutions of the equation

$$\begin{aligned}&[I_1 I_2 + m_2 l_1^2 I_2 - m_2^2 d_2^2 l_1^2]\omega^4 \\ -&[m_1 g d_1 I_2 + m_2 g l_1 I_2 + m_2 g d_2 I_1 + m_2^2 g d_2 l_1^2]\omega^2 \\ &+ m_1 m_2 g^2 d_1 d_2 + m_2^2 g^2 d_2 l_1 = 0. \end{aligned} \tag{2.11}$$

The question remains: is it reasonable to suggest that the analyitical treatment of a real and often chaotic system to be valid? That is the goal of the following section.

## 2.3 Measure twice, cut once: *Practical applicaton*

If we successfully characterize our double pendulum, that is, measure the mass, length, center of mass, and moment of inertia, of each pendulum we can use Equation 2.11 to predict the normal mode frequencies for small oscillations. Then, using the double pendulum apparatus we can measure the actual normal modes and compare to the theory.

Using a balance, a ruler, and some ingenuity, we determine the characteristics in Table 2.1. For the center of mass we hang the pendulum from its multiple hang points and compare it to a plumbline. Each orientation is marked on the pendulum arm. The intersection of the marks is the center of mass and the distance from the pivot to this intersection is $d_1$

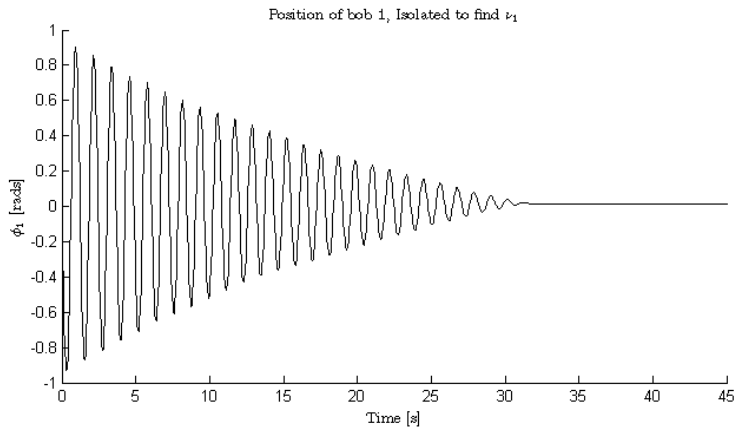


Figure 2.2: Motion of inner bob with the outer bob removed. This should yield the characteristic freqency (Figure 2.3) of the inner pendulum. By evidence of the envelope, we see that the inner pendulum shown here is more severely damped by friction than the outer pendulum in Figure 2.4.

and $d_2$ in Table 2.1. For the moment of inertia we find the natural frequency ($\nu$) of each pendulum by isolating it and letting it swing (the data sets in Figures 2.2 and 2.4). Then, the frequency of this motion is found using a Fast Fourier Transform (the results shown in Figures 2.3 for $\nu_1$ and 2.5 for $\nu_2$). Using the distance to center of mass ($d$), the mass ($m$), and the natural frequency ($\nu$), 2.12 is used to determine the moment of inertia ($I$).

$$\nu = \pi\sqrt{\frac{I}{mgd}} \Rightarrow I = \frac{mgd}{(2\pi\nu)^2} \tag{2.12}$$

Using Wolfram Mathematica, the values in Table 2.1 are plugged into Equation 2.11 to find the theoretical frequencies of the normal modes $\nu_+ = 1.62$ Hz and $\nu_- = 0.696$ Hz.

## 2.4 Compare to the Real Thing

Now, to answer the question, "Does our approximation hold?" Using the apparatus in Figure 3.4 we take an arbitrary motion of smallish oscillations shown in Figure 2.6 (though predominately in-phase motion). Note that this motion is real and is collected using

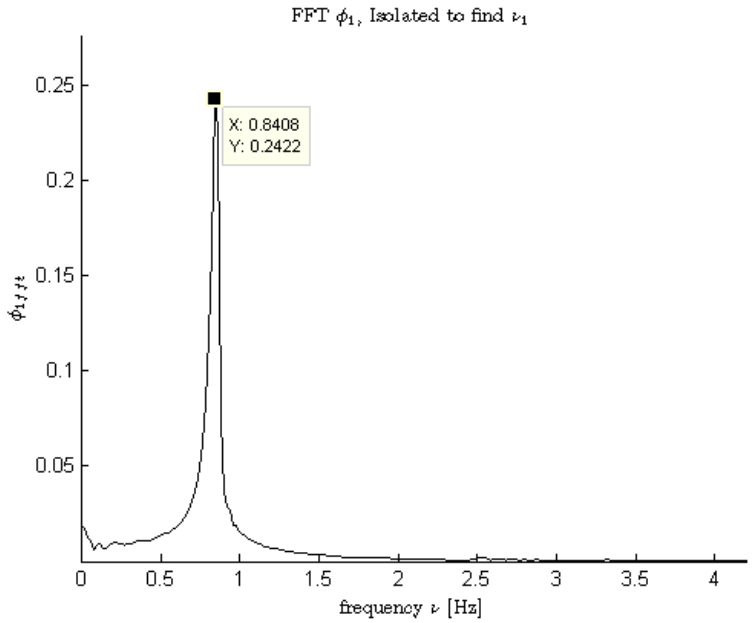


Figure 2.3: Fast Fourier Transform of the data in Figure 2.2. The peak frequency is the characteristic frequency of just the inner bob.

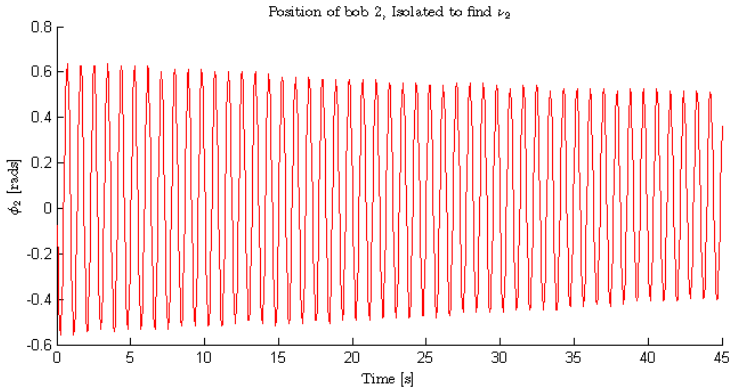


Figure 2.4: Motion of outer bob with the inner bob held fixed. This should yield the characteristic freqency (Figure 2.5) of the outer pendulum.

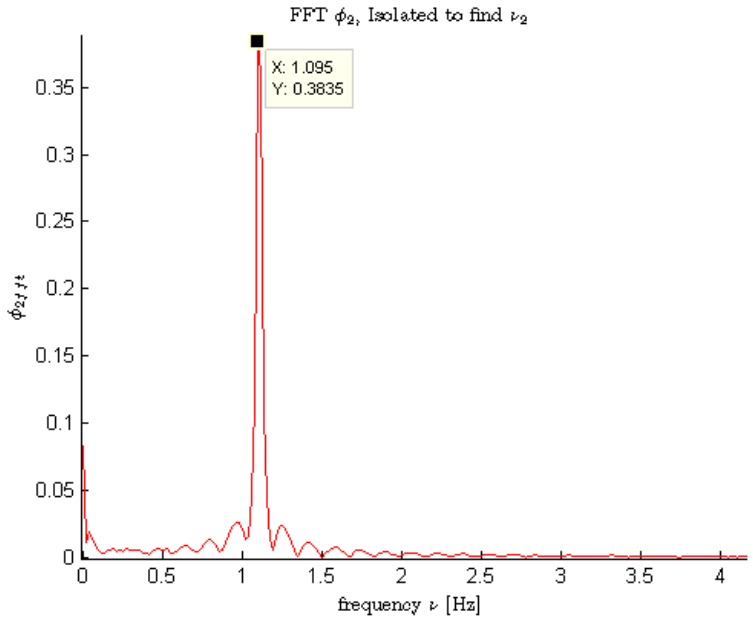


Figure 2.5: Fast Fourier Transform of the data in Figure 2.4. The peak frequency is the characteristic frequency of just the outer bob.

| Characteristic | value | |
|---|---|---|
| $m_1$ | 336.0 | g |
| $l_1$ | 43.5 | cm |
| $d_1$ | 21.0 | cm |
| $\nu_1$ | 0.83 | Hz |
| $I_1$ | 0.0254 | kgm$^2$ |
| $m_2$ | 202.2 | g |
| $l_2$ | 29.5 | cm |
| $d_2$ | 14.2 | cm |
| $\nu_2$ | 1.1 | Hz |
| $I_2$ | 0.00589 | kgm$^2$ |

Table 2.1: The characteristics of the Double Pendulum as measured the old fashioned way. $m$ is mass, $d$ is distance from axis of rotation to center of mass (center of mass found using plumbline comparison), $l$ is length of arm, $\nu$ is the natural frequency of the pendulum when isolated, and $I$ is the moment of inertia found using Equation 2.12 and data from Figures 2.3 and 2.5.

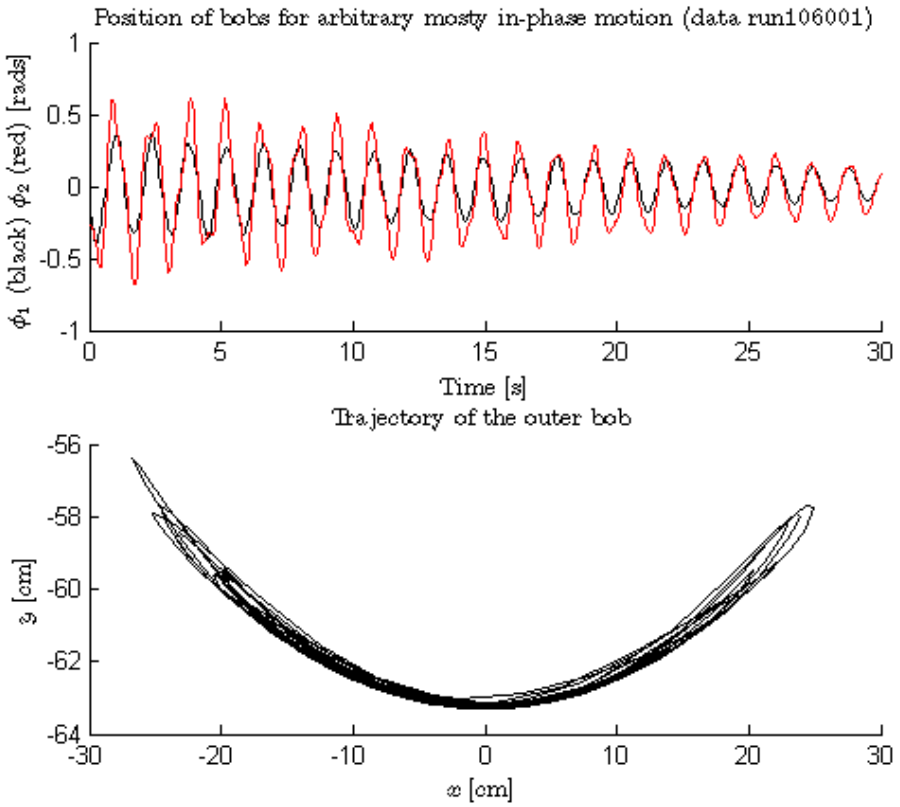


Figure 2.6: Position of bob (1) and bob (2) of the double pendulum released so that arbitrary motion with approximately small angles is acheived. This motion is predominately in-phase, though there are significant variations in $\phi_2$ especially.

LoggerPro/LabPro and the angles correspond to the angles in figure 2.1. The Fast Fourier transform of this position data (Figure 2.7) shows two peaks. One at $\nu_1 = 1.62$ Hz and the other at $\nu_2 = 0.724$ Hz which seem to correspond to $\nu_+$ and $\nu_-$ predicted in section 2.3, (1.62 Hz, 0.696 Hz).

Another data set yields more evidence of successful modeling. The motion described in Figure 2.8 and the FFT of this motion in Figure 2.9 yields frequencies $\nu_1 = 1.59$ and $\nu_2 = 0.724$ Hz. These are very similar to the previous data set.

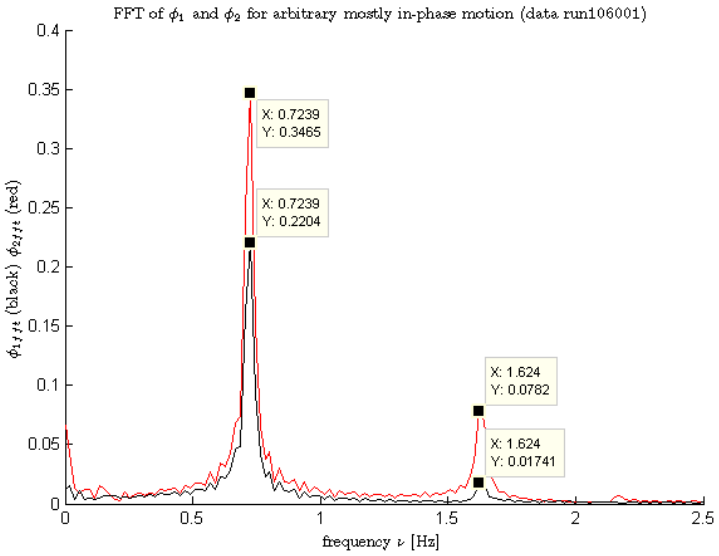


Figure 2.7: The FFT of the motion shown in Figure 2.6 for both $\phi_1$ and $\phi_2$. Peaks are the prominent frequencies in the motion and are $\nu_1 = 1.62$ and $\nu_2 = 0.724$ Hz.

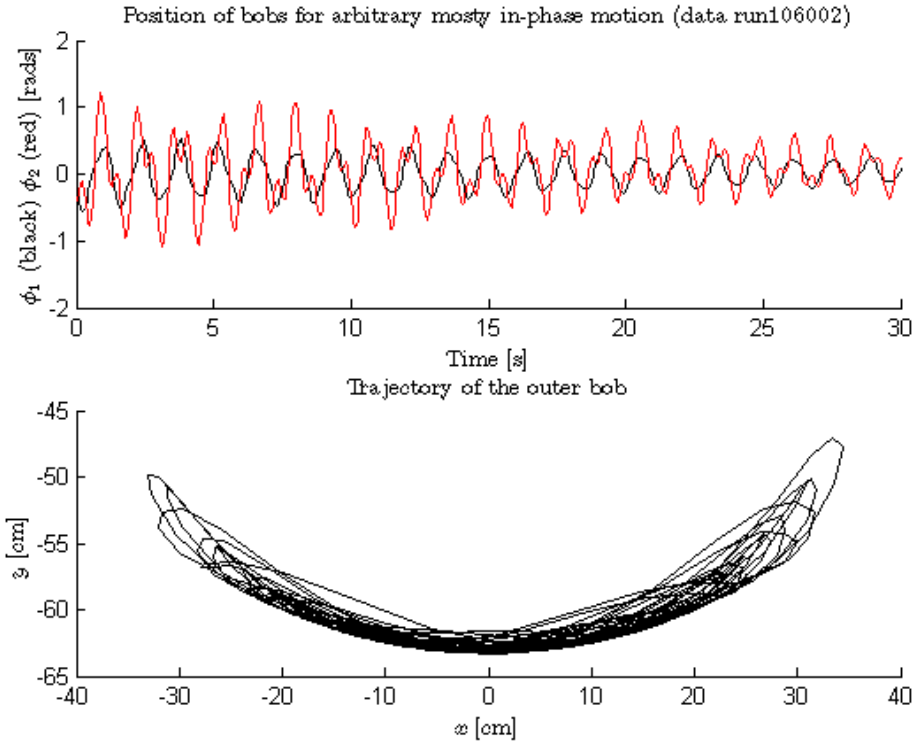


Figure 2.8: Another arbitrary motion with approximately small oscillations.

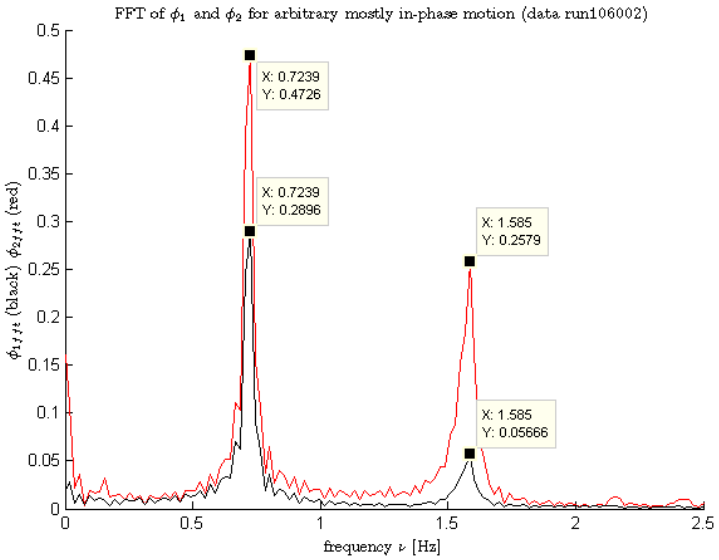


Figure 2.9: The FFT of the motion described in figure 2.8 for both $\phi_1$ and $\phi_2$. Peaks at $\nu_1 = 1.59$ and $\nu_2 = 0.724$ Hz.

## 2.5 Further Study

There are many avenues for further study with this apparatus. Besides updating the apparatus itself as outlined in Section 3.4, the theory can be continued by determining the eigenvectors that accompany these eigenvalues (the normal mode frequencies found above) to fully evaluate the normal modes. Also, one can explore numerical approaches to solving the equations of motion in Equation 2.10 (but without the approximations) and compare the findings to the actual motion of the Double Pendulum. The characteristics in Table 2.1 would help this endevor. One could do a full energy analysis to determine the quality factor of the coupled oscillators in the Double Pendulum or, better yet, determine a modification to the Equations of motion in Equation 2.10 to account for friction (is it constant, linear, quadratic...?). The ease of data taking with the double pendulum apparatus should allow for easy confirmation of appropriate friction models. Lastly, see additional papers on dynamic coupled oscillators like these in the American Journal of Physics. [5] [6] [7]

# Chapter 3

# Design and Construction

## 3.1 Goals and Features

We set out by determining the qualities our apparatus needed to have. The paramount concern: it needed to work. Preferably it needed to be easy to use, output live data, be sturdy and expandable, and be an improvement on previous iterations. In order to be straightforward to analyze, it needed to be confined to two dimesions and be relatively friction free. The predecessor pendulum shown in Figure 3.1 had wires that inhibited the inner arm from making complete revolutions. We wanted to improve this so higher energy states could be observed- states where the pendulum arms both completed full revolutions. The rotary motion sensors need to communicate wirelessly with the computer or there must be a clever wiring scheme to maintain electrical contact with the sensors without inhibiting motion.

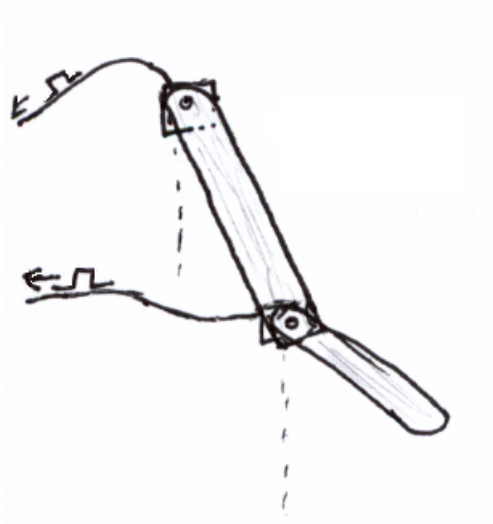

Figure 3.1: The previous iteration of a double pendulum using wooden arms and US Digital S1 rotary motion sensors.

## 3.2 Abandoned Avenues

The best option for wireless comunication seemed to be XBee [3] wireless devices, commonly incorporated with Arduino microprossesor boards. These devices are programmable via a personal computer and communicate with each other. The downside is that each sensor would need its own XBee to act as a sender and the computer would need one or two to act as receiver. At minimum, we would need three XBees. This option was abandoned in favor of a wiring scheme for simplicity.

The motion of the arms (or bobs) could be tracked a few different ways. The two options we considered were accelerometers and rotary motion sensors. Accelerometers have the advantage of measuring the motion wherever they are, but this is also a disadvantage because there would need to be an accelerometer on the outer arm of the double pendulum. Either wires would have to cross a second axle to the lower arm or a power source and wireless device would have to be mounted on that arm. Then the positions and angles would have to be calculated from the complicated acceleration data. Rotary motion sensors have the advantage of tracking the angle, the quantity that is most commonly solved for by

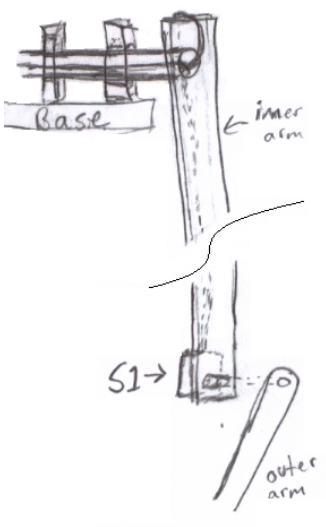


Figure 3.2: A sketch of the double pendulum in the planning stages. The key feature of the design is the wiring scheme.

convention. Additionally, the rotary motion sensor of the outer arm is not mounted on the outer arm but the inner arm and there is no reason for wires or power supplies to be mounted on this outer arm. As the simpler solution comes from using rotary motion (US Digital S1) sensors, that is the path chosen here.

## 3.3 Construction Details

### 3.3.1 Overall Design

First off, the design is based around solving the wiring problem. Wires need to get from the sensor (which serves as the axle for the outer arm) on the back of the inner arm up to the computer. As shown in Figures 3.2 and 3.3, the arm is given a hollow axle, which allows the wires to pass through to a handset cord detangler, commonly used on long coiled telephone handset cords and available at electronics stores. This scheme allows both arms to complete multiple rotations without losing electrical connection. The rotary motion sensor that reads the position of the inner arm can be attached to the axle by an elastic

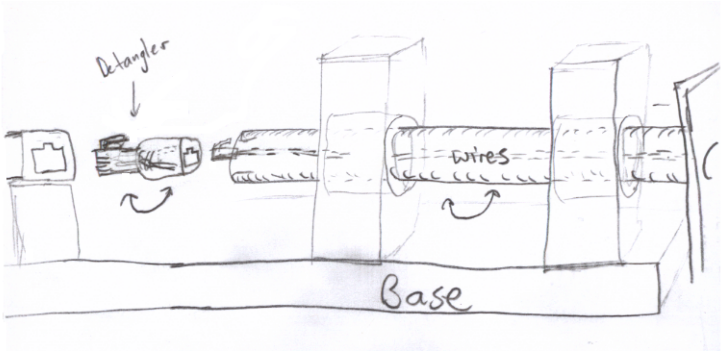


Figure 3.3: A sketch of the axle and detangler in design.

or rubber belt as shown in Figure 3.5.

The axle is 2024 alloy aluminum (0.50 in. OD and 0.34 in. ID) and is welded to the inner arm, also aluminum (of unknown alloy). The axle rotates with the aid of two bearings (0.50 in. ID) mounted in hand-made wooden pillow blocks (Brazillian epi, hard wood). The epi allows for long holes along its long dimension so that the pillow blocks can be bolted to the base (3/4 in. 6-ply wood).

### 3.3.2 Wiring and Circuit

The use of the handset detangler in Figure 3.3 provides an excuse to use telephone and ethernet cables and connectors for easy wiring and accessability. Each S1 gets a handset cable for power and signal output (4-wires- +5, gnd, **A**, and **B**). The S1 sensor from US Digital is not directly compatible with the Vernier Labpro. The LabPro wants to see pulses on one channel for clockwise and another channel for counter-clockwise. Instead, the S1, as an optical rotary motion sensor, outputs pulses on both channels **A** and **B** as shown in Figures 3.6 and 3.7. In order to fix this, the signal must be translated.

The custom circuit in Figure 3.8 performs this translation. Pulses on channels **A** and **B** from the S1s correspond to a fixed number of radians (about 500 pulses per $2\pi$ radians). These pulses are 90 degress out-of-phase. What distingushes clockwise from

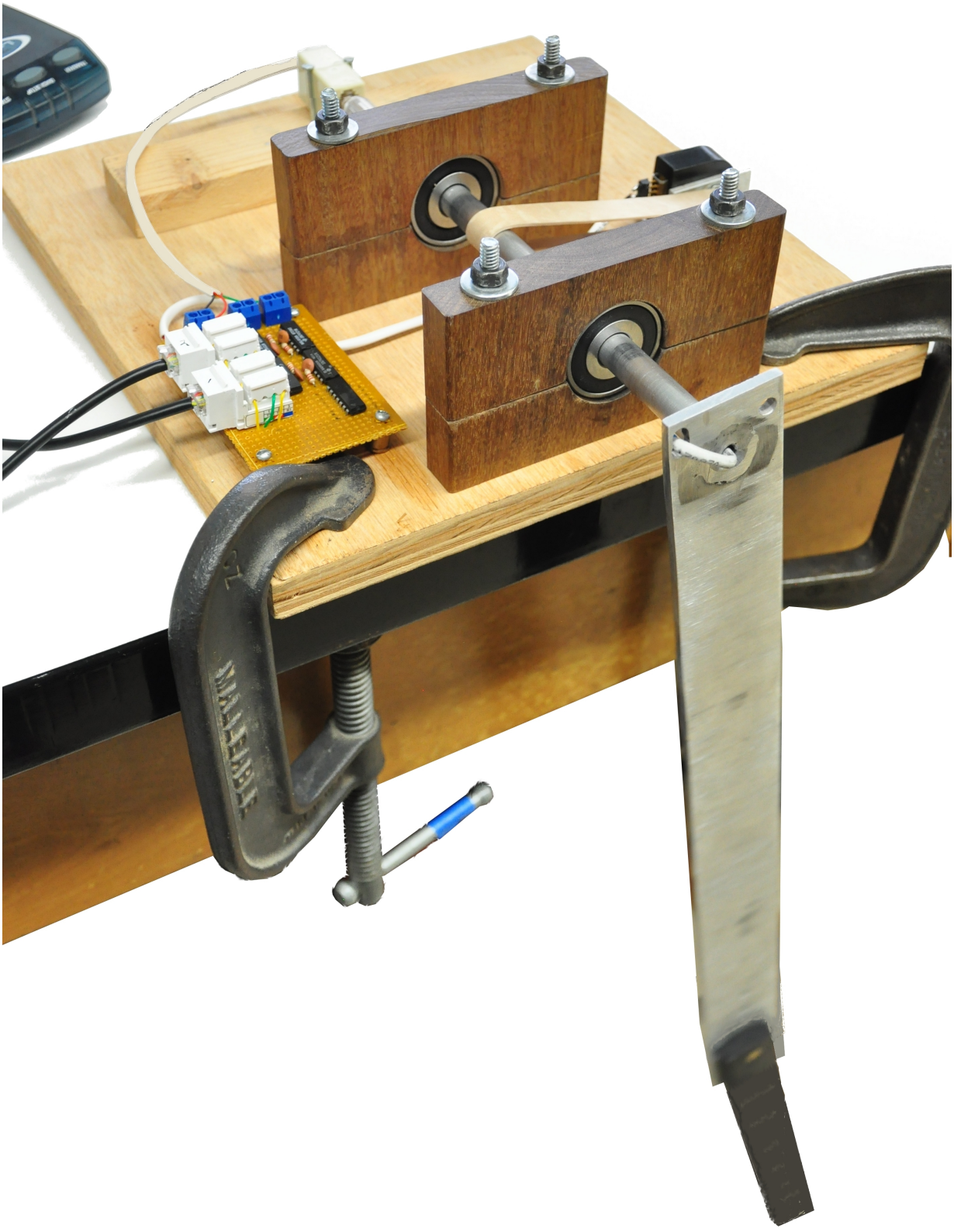

Figure 3.4: The double pendulum aparatus.

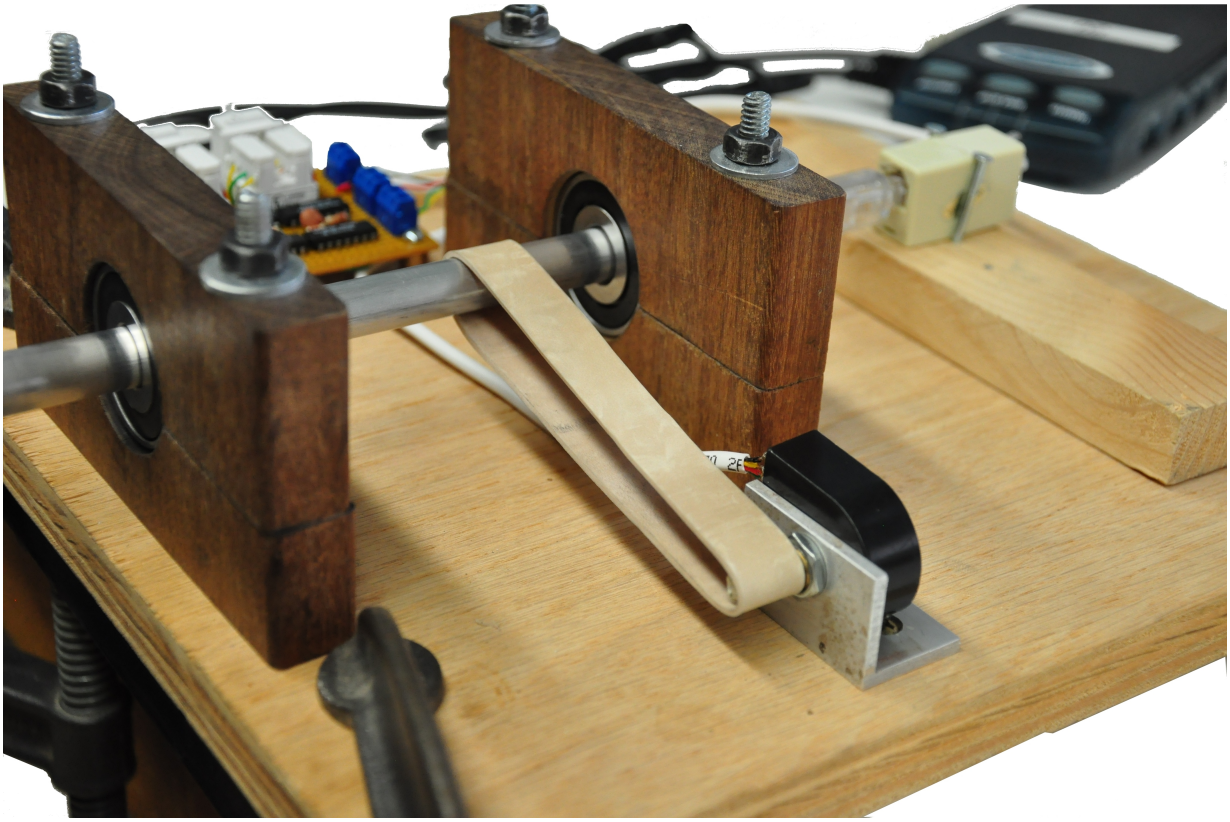

Figure 3.5: The double pendulum apparatus from the side, showcasing the belt and the belt-driven S1 rotary motion sensor for the inner bob (1).

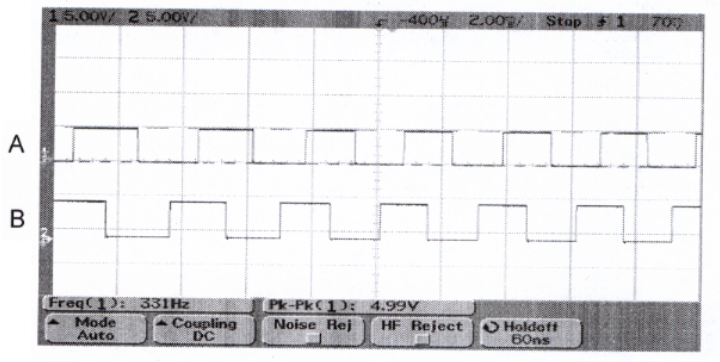


Figure 3.6: The signal output by a US Digital S1 for clockwise rotation.

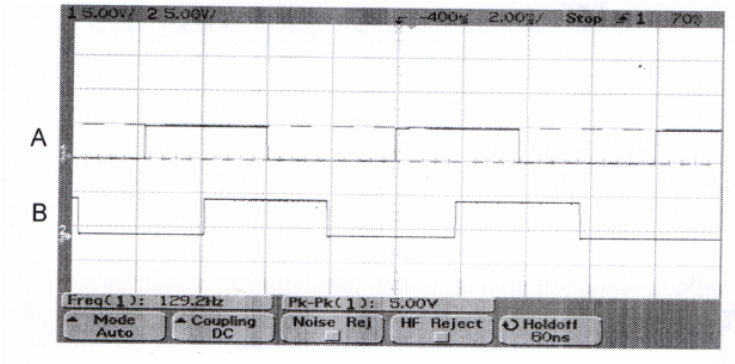


Figure 3.7: The signal output by a US Digital S1 for counter-clockwise rotation (slightly slower rotation than Figure 3.6).

counter-clockwise rotation is which pulse leads. Figures 3.6 and 3.7 show this difference in leading pulses. The translator circuit checks to see which channel pulse is leading. Figure 3.9 shows these pulses in the translator circuit. If **A** is leading, **A** triggers a pulse from a one-shot that is sufficiently narrow so that it is unlikely two adjacent pulses will overlap. This pulse (**QA**) is compared with **B** at an AND-gate. If **B** is high, then **B** leads **A** and the AND-gate (**QA+B**) outputs high (a pulse is allowed to pass). If **A** leads, then **B** is low and **QA+B** remains low (no pulse is passed). Instead, when **B** triggers a one-shot pulse (**QB**) that is compared to **A**, (**QB+A**) goes high (a pulse is allowed to pass), telling the LabPro that the S1 rotary motion sensor is rotating counter-clockwise. A photo of the circuit on the apparatus is included in Figure 3.10.

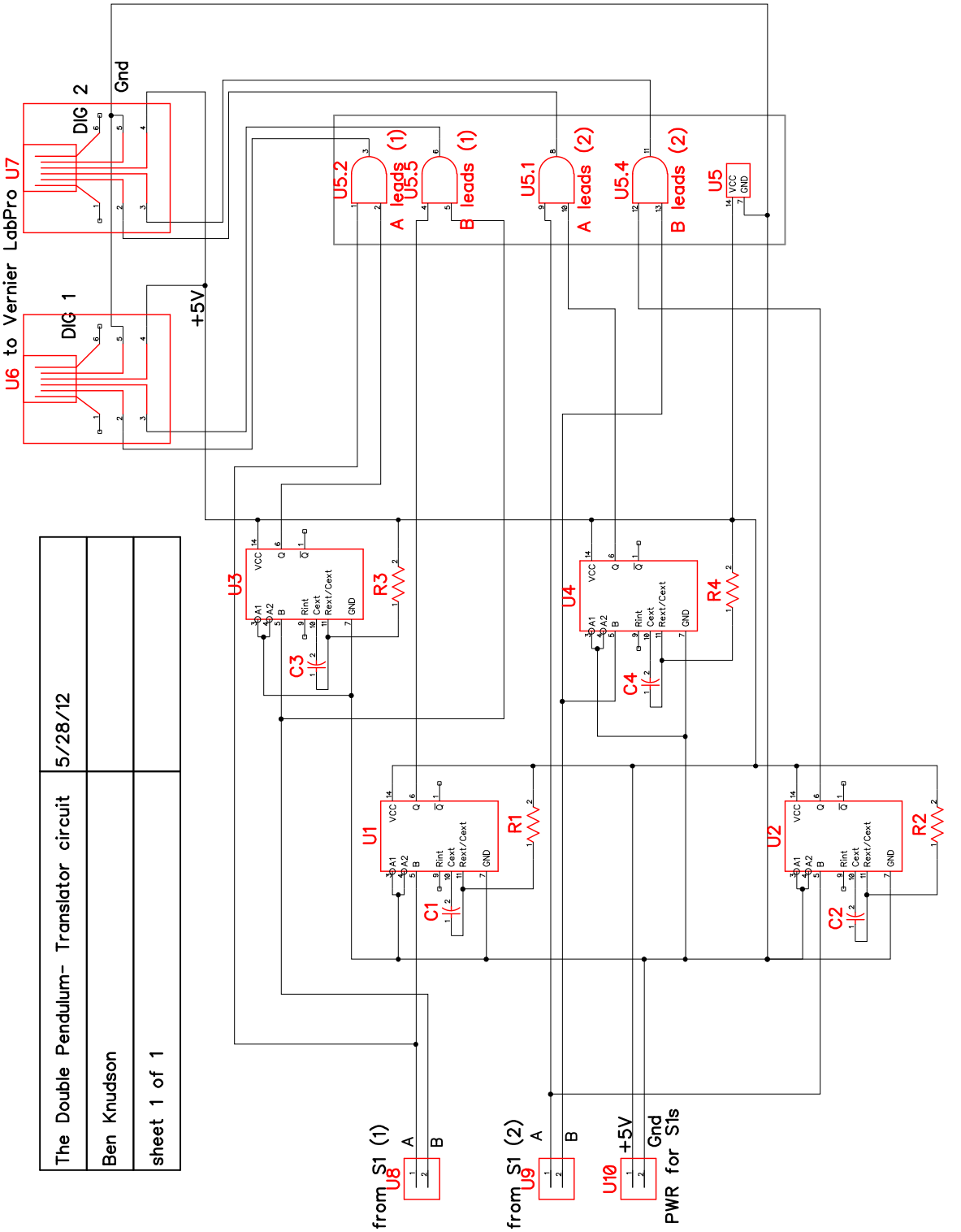


Figure 3.8: The circuit that translates the signal from each US Digital S1 to a Vernier-friendly format (pulses for clockwise on one channel and pulses for counter-clockwise on another channel).

| Reference designation | component | value |
|---|---|---|
| U1,U2,U3,U4 | SN74121N | one shot |
| U5 | 74F08 | 4 AND-gate |
| U6,U7 | ethernet port | 6-wire |
| U8,U9,U10 | raw wire connect | |
| R1,R2,R3,R4 | resistor | 2.2 $\pm$5% $k\Omega$ |
| C1,C2,C3,C4 | capacitor | 0.010 $\pm$10% $\mu F$ |

Table 3.1: Legend of the Components in Figure 3.8. Choose the values of capacitors and resistors such that the up-pulse widths from the SN74121Ns are 10-100$\mu$s. This avoids false positives during particularly fast rotations- when the pulses on **A** and **B** in Figures 3.6 and 3.7 are particularly short and close together.

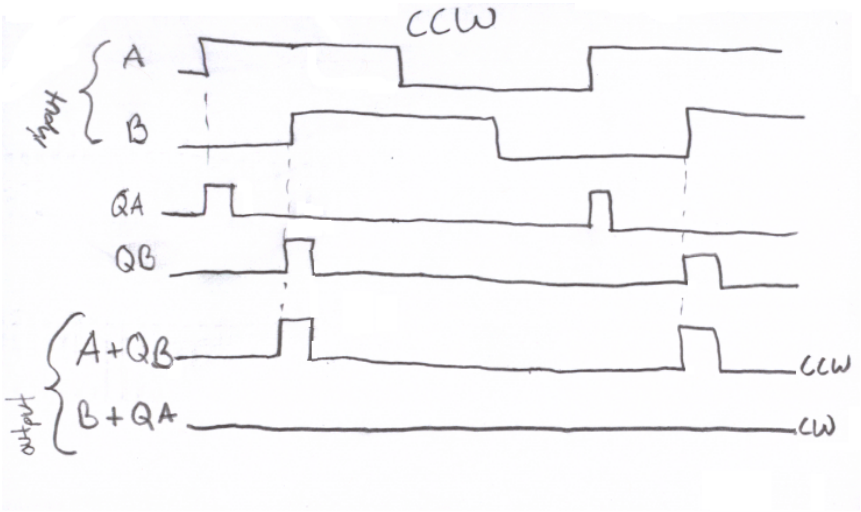


Figure 3.9: The pulse-train diagram of the circuit in Figure 3.8 for counter-clockwise rotation. Only one motion sensor input/output is shown.

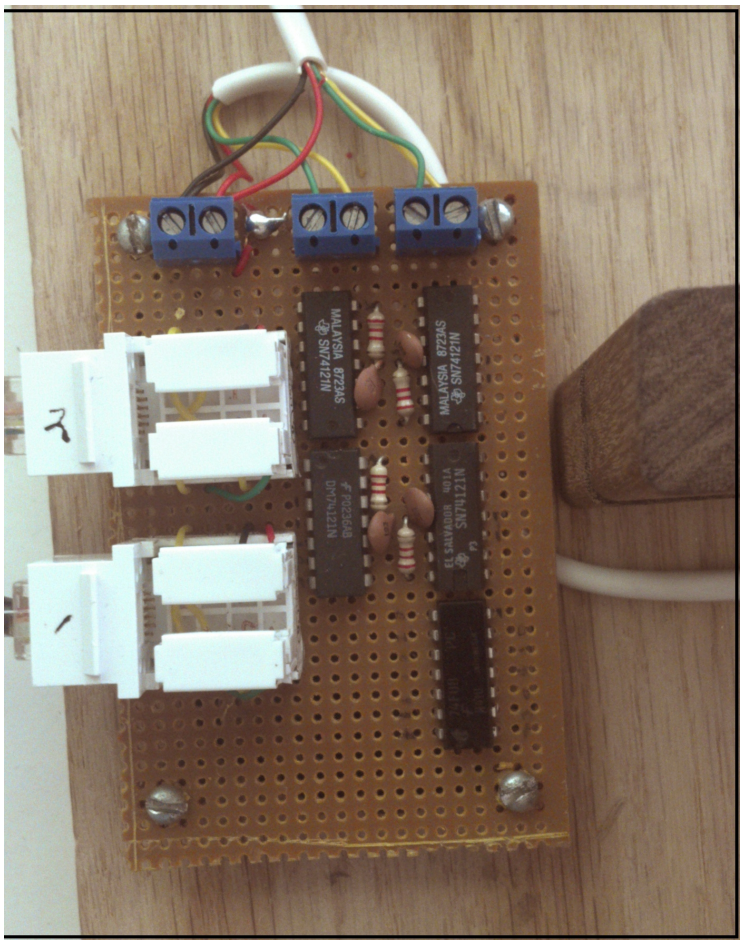


Figure 3.10: The translator circuit mounted on the base of the double pendulum.

## 3.4 Design Improvements for Future Iterations

Having built the Double Pendulum and looking back, there are a few things I would have done differently. The goal was to create an apparatus that was adjustable, but the inner arm is welded to its axle. If, instead, a bracket was welded to the axle, then multiple inner arms could be fabricated and used with this apparatus. This axle could be made using the surplus 2024 aluminum tube. The current iteration, though relatively friction-free, *clangs* when the outer arm swings past the inner arm. This does not impead the motion of the double pendulum significantly, but it can still be fixed with a more ridged scheme. The translator circuit currently on on the apparatus is a prototype with crude assembly. Apendix A outlines a method for assembling a more elegant circuit.

# Chapter 4

# Using the Double Pendulum

## 4.1 Lab Connections

The double pendulum apparatus is designed to work seamlessly with a Vernier LabPro interface and LoggerPro software. The wires from the pendulum have Vernier British Telecom connectors which connect to the digital ports of a LabPro. (Both ports are needed, one for each sensor which is how LoggerPro expects rotary motion sensors to be attached. If one is willing to convince LoggerPro to use all of its digital channels [four per port], it is possible for one LabPro to read data from four motion sensors- two on each port- since each sensor requires two digital channels, one for each direction clockwise + and counter-clockwise−.)

Other options include using a Vernier LabQuest as a lab interface, which has the added benefit of being mobile and battery-powered. The LabPro is also compatible with National Instruments LabView and a VI that is ready for rotary motion sensor data collection can be obtained from the Vernier website and subsequently customized.

## 4.2 LabPro and LoggerPro

Run the LoggerPro `.cmbl` file included (`Double Pendulum.cmbl`). This will open a user interface like the one shown in Figure 4.1. If the `Rotary Motion Sensors` are not recognized upon opening the `.cmbl` file, make sure the LabPro has power and the double pendulum cables are plugged into the `DIG 1` and `DIG 2` ports. Connect the LabPro to LoggerPro by accessing **Experiment > Connect Interface** and sellecting LabPro. After connecting the LabPro, set up the sensors by accessing **Experiment > Set up Sensors**. The LabPro should appear. On the `DIG 1` and `DIG 2` ports, right-click and choose **Rotary Motion Sensor** from the drop down menu and un-check the option for the sensors to `Zero on Collect`. Now Calibrate the sensors.

### 4.2.1 Calibration

Each sensor outputs pulses as it rotates, but these do not directly correspond to degrees or radians until we calibrate each sensor. The sensor on the lower arm serves as its axle, but the sensor on the upper arm is attached to the (larger-diameter) axle via a rubber band. Automatic calibration is not possible because of the custom nature of the apparatus. Go to **Experiment > Calibrate** for each sensor. Confirm that under the equation tab the sensor attached to the inner arm (marked as 1 on the apparatus) is set to 935 pulses/rotation in units of Rads and that the sensor attached to the outer arm (marked as 2 on the apparatus) is set to 510 pulses/rotation in units of Rads. These calibrations are approximate and should yeild two significant figures of accuracy. The user is encouraged to determine more exact calibrations as needed.

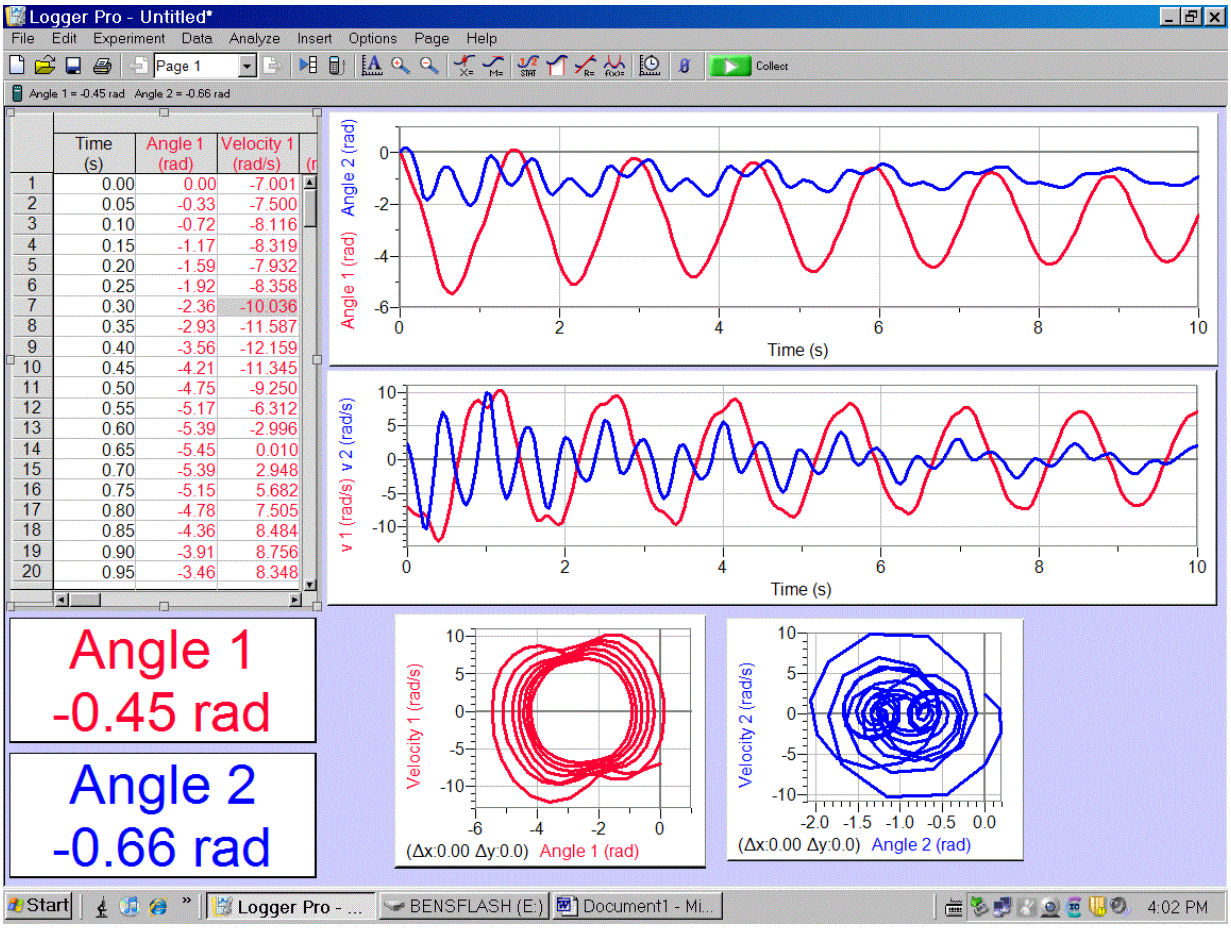


Figure 4.1: Screenshot from Double Pendulum.cmbl in Vernier LoggerPro.

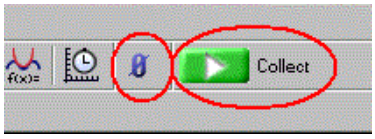


Figure 4.2: The zero (left) and collect (right) buttons in LoggerPro.

### 4.2.2 Zeroing and Triggering

When using LoggerPro to obtain data, it is important to notice its weaknesses. During the time immediately before and after data collection, LoggerPro tends to stop paying attention. If the double pendulum is moving during this time, it is likely that LoggerPro will lose track of where zero is. It is good practice to zero between each data collection. Place the double pendulum so that its two arms hang vertically at rest and click the `zero` button shown in Figure 4.2. Since the double pendulum must be stationary when you click `Collect` to avoid a floating zero, you have two options for data collection.

1. Click `Collect`, wait, and then move the double pendulum to get it started in the motion for which you wish to collect data. This method is not repeatable and some of your data will show the time when the arms were stationary and then when they were being manipulated. If more consistent data is desired, use the second option.

2. Set the Triggering option "on" by going to **Data > Data Collection** or by pressing **CTRL+D**. Turn on `Triggering` and on the **Triggering** tab select the parameters for triggering (e.g. If you wish to collect data on several releases from both arms located at $\frac{\pi}{4}$, then perhaps set the trigger to be "sensor #1 decreasing value through 0 rads." Then, to impelment this triggering, `zero` the sensors and click `Collect`. LoggerPro will now display a **Waiting for triggered data** message. Now place the double pendulum in your desired starting position taking care not to allow sensor #1 to trigger data collection and then release from this position).

# Acknowledgements

I would like to thank Matthew Moelter, David Arndt, James Hilsinger, Taylor Post, and Samuel Meijer for their contributions to this project.

# Bibliography


[1] S. H. Strogatz, *Nonlinear Dynamics and Chaos*. Perseus Books Publishing, LLC. 1994.

[2] J. R. Taylor, *Classical Mechanics*. University Science Books. Sausalito, CA, 2005.

[3] See `http://www.digi.com/xbee/` for information on XBee transducers.

[4] Data sets taken by Taylor Post, Department of Physics, Cal Poly.

[5] P. Ramachandran, S. G. Krishna, and Y. M. Ram, "Instability of a constrained pendulum system", Am. J. Phys. **79** (4), 395 (2011).

[6] M. Z. Rafat, M. S. Wheatland, and T. R. Bedding, "Dynamics of a double pendulum with distributed mass", Am. J. Phys. **77** (3), 216 (2009).

[7] R. B. Levien, S. M. Tan, "Double Pendulum: An experiment in chaos", Am. J. Phys. **61** (11), 1038 (1993).

# Appendix A

# Translator Circuit

Here is a trace of the circuit in Figure 3.8 so that a proper version can be manufactured using a double-sided copper trace board available at electronic supply stores. Holes for the ICs and components can be drilled according to the diagram. Then, the traces can be drawn with a Sharpie and the rest of the copper removed with etchant. The traces shown in Figures A.1 and A.2 are thinner than you would make using a Sharpie. Thicker traces are not a problem as long as shorts and breaks are avoided. The traces provided are the proper size for the DIP components in Table 3.1. Figures A.3 and A.4 show what the printed circuit boards would look like if they were manufactured professionally and are provided as eye-candy.

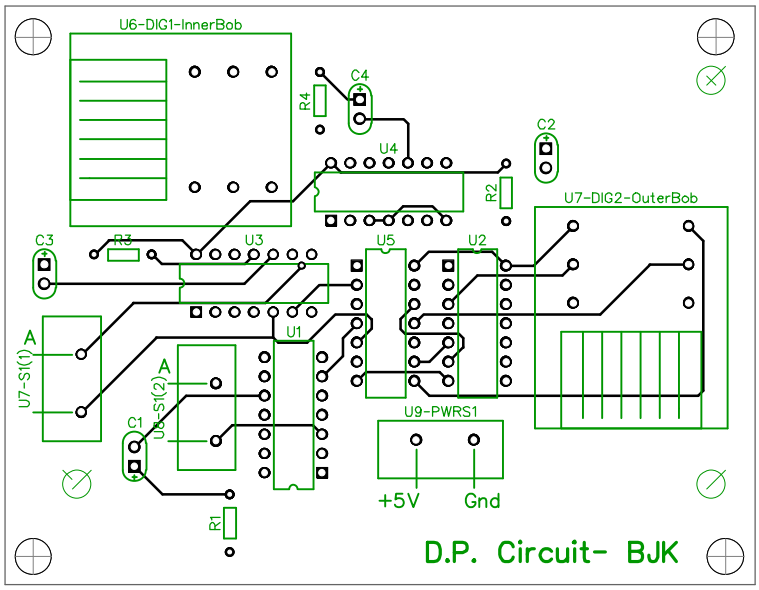


Figure A.1: The top layer of printed circuit board for the translator circuit designed in DipTrace.

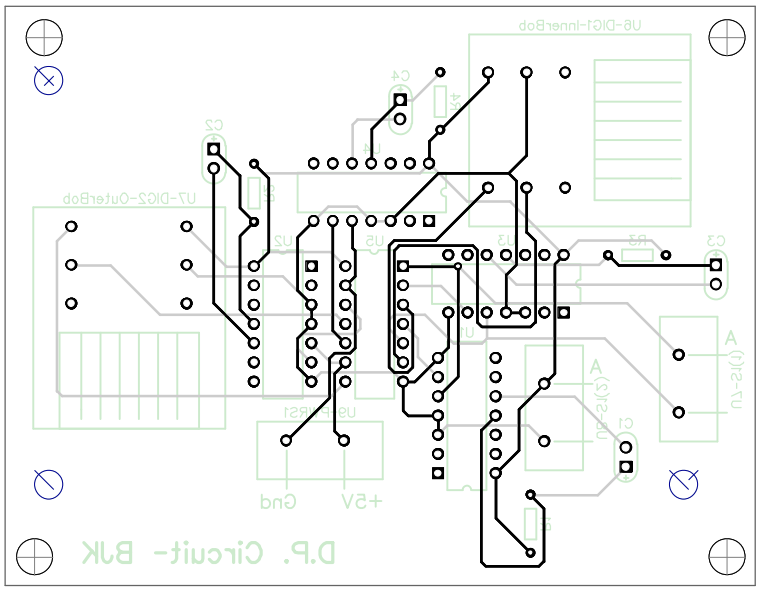

Figure A.2: The bottom layer of printed circuit board for the translator circuit designed in DipTrace.

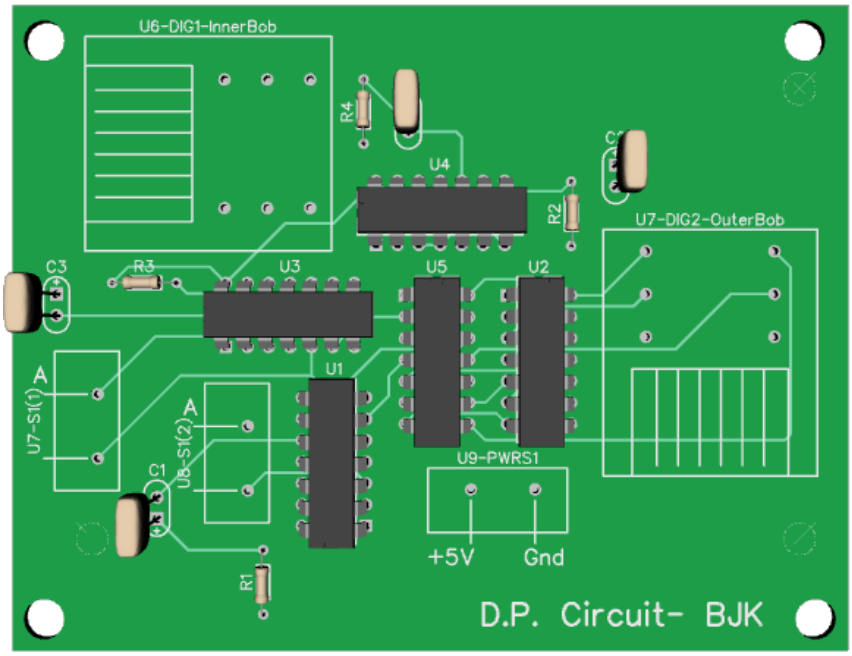


Figure A.3: The top of the translator circuit as rendered by DipTrace.

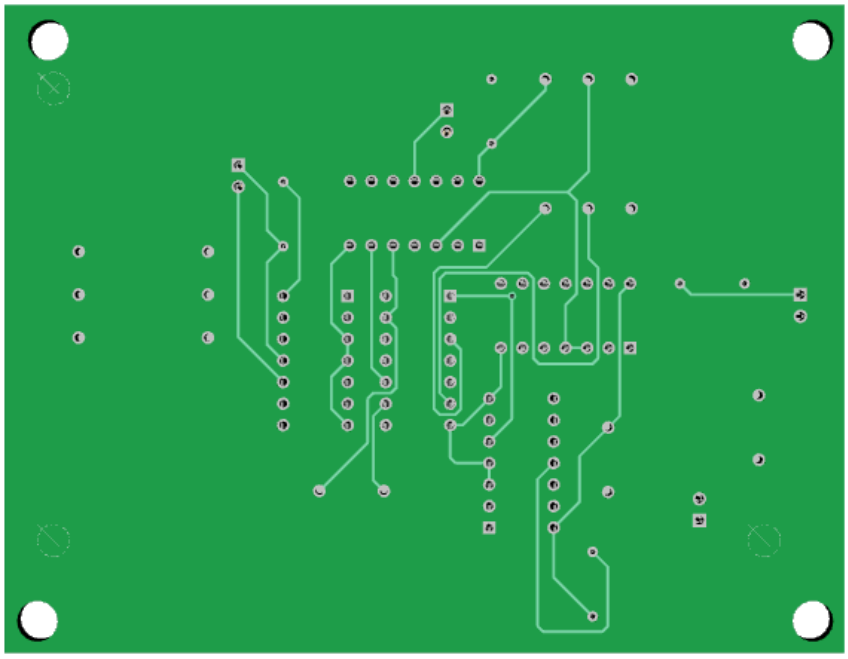

Figure A.4: The bottom of the translator circuit as rendered by DipTrace.

# Appendix B

# Additional Data Sets

These data sets in Figures B.1 and B.2 showcase chaos. Initial conditions are as consistant as we can make them, yet the motions that result are quite different. Some patterns and similarities are evident, but the trajectories are more or less distributed accross the space provided. Note: These data sets were collected using the higher-fiction set-up to reduce state-space, which is an option of the Double Pendulum.

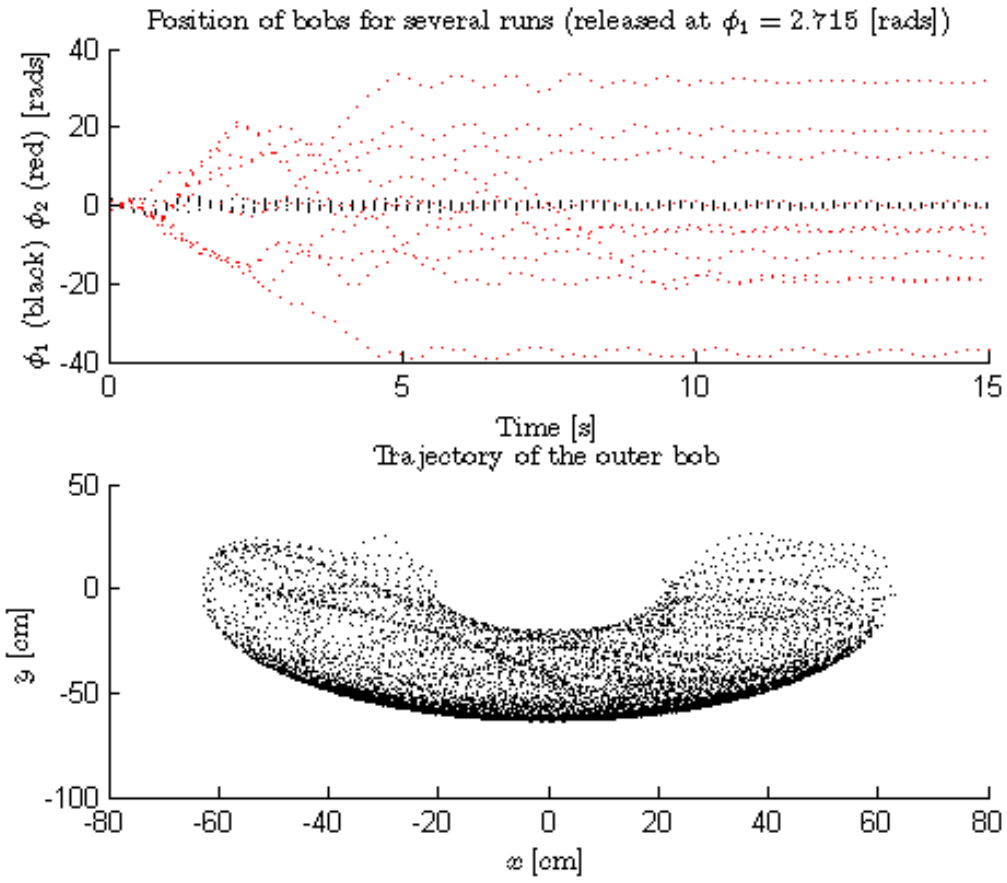


Figure B.1: Data for several runs starting with the inner bob at 2.715 rads. [4] (Runs 1-10)

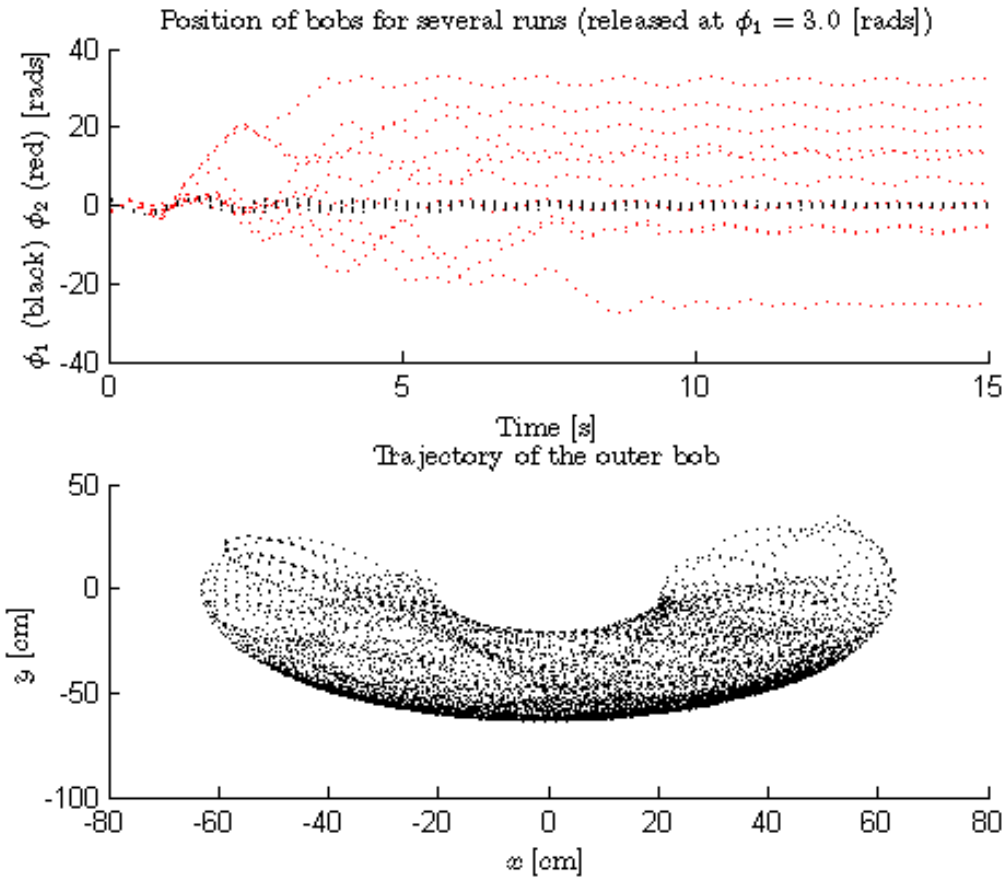


Figure B.2: Data for several runs starting with the inner bob at 3.0 rads. [4](Runs 21-30)

# Appendix C

# Matlab Code for Fourier transform

Filename `fftmaker.m` Matlab script

```
%417 fft of double pendulum
%bjknudso
%%
clear all
[filename,pathname]=uigetfile('*.*','load this data');
% this reads the file, creates a structure with headers and 'data'
%
contents=importdata(filename)
%
maxnumnf=length(contents.data);
time=contents.data(2:end,1);
theta1=contents.data(2:end,9);
theta2=contents.data(2:end,10);
y=contents.data(2:end,11);
x=contents.data(2:end,12);
%%
figure(2)
subplot(2,1,1) %(m,n,p) mxn is the divisions, and pth place in the array
hold on
plot(time,theta1,'k',time,theta2,'r')
xlabel('Time [s]','interpreter','latex')
ylabel('$\phi_1$ (black) $\phi_2$ (red) [rads]','interpreter','latex')
title('Position of bobs for high energy motion (data run107001)','interpreter','latex')
hold off
subplot(2,1,2)
hold on
plot(x,y,'k')
title('Trajectory of the outer bob','interpreter','latex')
```

```
xlabel('$x$ [cm]','interpreter','latex')
ylabel('$y$ [cm]','interpreter','latex')
hold off
%%
l=size(time);
L=l(1);
Fs=L/(time(end)-time(1));
NFFT = 2^nextpow2(L); % Next power of 2 from length of y
Theta1 = fft(theta1,NFFT)/L;
Theta2 = fft(theta2,NFFT)/L;

f = Fs/2*linspace(0,1,NFFT/2+1);
figure(1)
hold on
title('FFT of $\phi_1$ and $\phi_2$ for high energy motion (data run107001)',...
      'interpreter','latex')
xlabel('frequency $\nu$ [Hz]','interpreter','latex')
ylabel('$\phi_{1fft}$ (black) $\phi_{2fft}$ (red)',...
'interpreter','latex')
plot(f,2*abs(Theta2(1:NFFT/2+1)),'r',f,2*abs(Theta1(1:NFFT/2+1)),'k')
hold off
```

# Appendix D

# Mathematica functions

Filename DP. Mathematica Notebook

```
The Double Pendulum
An Interesting Dynamic System
Ben Knudson
Senior Project and PHYS 417 project

Normal modes
g=9.8;
m1=0.336;
m2=0.2022;
l2=0.295;
l1=0.435;
d1=0.21;
d2=0.142;
f1=0.83;
f2=1.1;
l2;
I1=m1*g*d1/((2 *Pi*f1)^2)
I2=m2*g*d2/((2 *Pi*f2)^2)

\[Phi]1;
\[Phi]2;
\[Omega]01;
\[Omega]02;

0.0254255
0.00589048

Simplify[(d2*g*I1*m2 + d2*g*l1^2*m2^2 + g*I1*m1 + g*I2*l1*m2) \[PlusMinus]
   Sqrt[(2*(d2^2*l1^2*(-m2^2) + I1*I2 + I2*l1^2*m2))*
```

```
     ((d1*g*I2*m1 + d2*g*I1*m2 + d2*g*l1^2*m2^2 + g*I2*l1*m2)^2 -
      4*(d2^2*l1^2*(-m2^2) + I1*I2 + I2*l1^2*m2)*(d1*d2*g^2*m1*m2 +
        d2*g^2*l1*m2^2))]]
g (I1 (m1+d2 m2)+l1 m2 (I2+d2 l1 m2))\[PlusMinus]Sqrt[2]
*\[Sqrt](g^2 (I1 I2+l1^2 m2 (I2-d2^2 m2)) (-4 d2 m2 (d1 m1+l1 m2)
*(I1 I2+l1^2 m2 (I2-d2^2 m2))+(d1 I2 m1+m2 (I2 l1+d2 (I1+l1^2 m2)))^2))
Solve[(I1*I2 + m2*l1^2*I2 - m2^2*d2^2*l1^2)*\[Omega]^4 -
    (m1*g*d1*I2 + m2*g*l1*I2 + I1*m2*g*d2 + m2^2*g*d2*l1^2)*\[Omega]^2 +
    (m1*m2*g^2*d1*d2 + m2^2*g^2*l1*d2) == 0, \[Omega]]
{{\[Omega]->-10.21898521352089`},{\[Omega]->-4.370411567311167`},
{\[Omega]->4.370411567311167`},{\[Omega]->10.21898521352089`}}/(2*Pi)
{{-10.21898521352089`},{-4.370411567311167`},{4.370411567311167`},
{10.21898521352089`}}/(2*Pi)
{{-1.6264},{-0.695573},{0.695573},{1.6264}}
7.0428
3.1305
(5.7844/3.1305)^2
3.4142
(2.39598/3.1305)^2
0.585786

Simplify[(1/2)*I1*\[Phi]1'^2+(1/2)*m2*l1^2*\[Phi]1'^2+(1/2)*I2
*\[Phi]2'^2+m2*d2*l1*\[Phi]1'\[Phi]2'*Cos[\[Phi]1-\[Phi]2]
-(m1*g*d1*(1-Cos[\[Phi]1])+m2*g*(l1*(1-Cos[\[Phi]1])+d2*(1-Cos[\[Phi]2])))]
1/2 (2 g (-d1 m1-d2 m2-l1 m2+d1 m1 Cos[\[Phi]1]
+l1 m2 Cos[\[Phi]1]+d2 m2 Cos[\[Phi]2])+(I1+l1^2 m2) (\[Phi]1^\[Prime])^2
+2 d2 l1 m2 Cos[\[Phi]1-\[Phi]2] \[Phi]1^\[Prime] \[Phi]2^\[Prime]
+I2 (\[Phi]2^\[Prime])^2)
```